Application of the Finite-Element Method to One-Dimensional Flame Propagation Problems

D. N. Lee* and J. I. Ramos†
Carnegie-Mellon University, Pittsburgh, Pennsylvania

A linear semidiscrete Galerkin method and an adaptive finite-element method are first used to compute the steady-state wave speed of a reaction-diffusion equation which has an exact traveling wave solution. The Galerkin method is then applied to study the propagation of a laminar flame in a closed combustor. The numerical results obtained with the Galerkin and adaptive finite-element methods are compared to those obtained with a finite-difference Crank-Nicolson scheme. The comparisons show that the finite-element methods overpredict the wave speed, whereas the Crank-Nicolson scheme underpredicts it. The Galerkin method results are closer to the exact solution than those of the Crank-Nicolson scheme for a 901 point grid. The adaptive finite element requires about 171 points to obtain a wave speed equal to that of the Galerkin method with 901 points. The application of the Galerkin method to the propagation of one-dimensional enclosed deflagrations shows that, in order to account properly for the steep temperature gradients at the flame front, at least 400 grid points are required. The largest temperature difference between the finite-difference and finite-element results is less than 2%. This difference is attributed to the oscillations present in the finite-element method, the linearization of the reaction terms and the use of linear basis.

Nomenclature

a,b = matrices defined by Eqs. (40) and (41)
A = vector, Eq. (22) or scalar, Eq. (45)
C_p = specific heat at constant pressure
C_v = specific heat at constant volume
D = mass diffusivity
E = activation energy
H = sensible plus formation enthalpy
H^0 = enthalpy of formation
K = pre-exponential factor
L = combustor length, $L = 10$ cm
L_2 = norm defined by Eq. (44)
$\dot{m}$ = reaction rate
M = mass (per unit area) contained in the combustor
n = number of grid points
N = number of species
p = pressure
q = defined by Eq. (38)
Q = heat of combustion
R = specific gas constant
$\tilde{R}$ = univeral gas constant
s = stoichiometric coefficient
S = vector or reaction rate terms, Eq. (23)
t = time
T = temperature
u = velocity
V = wave speed
W = molecular weight, $W = 28.91$ g/mole
x = Eulerian coordinate
y = species mass fractions
α = diffusion coefficient, Eq. (18)
γ = ratio of specific heats, $\gamma = 1.4$
Δ = increment
μ = kinematic viscosity
ξ = Lagrangian coordinate
ρ = density
ϕ = variable defined in Eq. (10)
ψ = linear basis
$\dot{\omega}$ = reaction rate, $\dot{\omega} = \dot{m}/\rho$

Superscripts

k = iteration
n = time $t^{(n)}$
T = transpose

Subscripts

c = computed
i = grid points
j = species
ℓ = grid point
0 = reference value
$1,2,3,4$ = fuel, oxidizer, inert, and products

Introduction

THE propagation of premixed flames through confined mixtures has been the subject of various numerical investigations. Ramos[1] studied flame propagation in one-dimensional Cartesian coordinates. The problem was formulated in such a way that the momentum and overall continuity equations need not be considered. A transformation of independent variables reduced the governing equations of mass and energy to a system of reaction-diffusion equations, which were solved by means of nine finite-difference schemes. The relative advantages and disadvantages of these methods were assessed in terms of computational efficiency and accuracy.

More recently, Ramos[2,3] used finite-difference schemes to study the propagation of confined laminar flames in spherical and cylindrical coordinates. The governing equations were reduced to a system of integrodifferential reaction-diffusion equations. The numerical solution of these equations revealed that the accuracy and efficiency of a particular algorithm are rather sensitive to the problem nonlinearities and geometry under consideration. Moreover, in order to resolve the flame structure properly, a large number of grid points were required.

In the present paper an alternate numerical procedure is developed and applied to study the propagation of confined laminar flames. The method is a semidiscrete finite-element procedure which uses linear basis.

The development and application of finite-element methods to combustion problems in confined geometries seem to be new topics which have not been considered in the past. Margolis[4] used a time-dependent approximation to calculate the speed of a premixed ozone flame. He neglected the pressure variations and viscous dissipation and applied a

Presented as Paper 82-0035 at the AIAA 20th Aerospace Sciences Meeting, Orlando, Fla., Jan. 11-14, 1982; submitted Jan. 20, 1982; revision received May 28, 1982.

*Postdoctoral Fellow, Department of Mathematics.
†Assistant Professor, Department of Mechanical Engineering. Member AIAA.

Lagrangian spatial coordinate to reduce the governing equations to a system of reaction-diffusion equations for the temperature and species concentrations. He then introduced an appropriate B-spline (finite-element) basis for the spatial variation, collocation, and boundary conditions on the time-dependent coefficients and obtained a stiff ordinary initial value problem which was solved via a highly accurate method of lines. A method of lines with splines was also used by Otey and Dwyer[5] in their studies of the interaction between fast chemistry and diffusion. Heimerl and Coffee[6] modeled the ozone flame using variable properties and used a spline method to solve the governing equations of mass and energy. Margolis,[4] Otey and Dwyer,[5] and Heimerl and Coffee,[6] used the PDECOL code of Madsen and Sincovec,[7] while Sandusky et al.[8] developed a finite-element method for modeling combustion using a variable step size.

The present paper describes a finite-element method which is applied to a scalar reaction-diffusion equation.[9] This equation has an exact traveling wave solution with which the numerical results are compared. The method is then applied to study the propagation of confined laminar flames in Cartesian coordinates, and its results are compared with those obtained using a finite-difference scheme. An adaptive finite-element method is also developed and applied to compute the wave speed of a scalar reaction-diffusion equation. This method offers a promising approach to the resolution of high gradient regions in combustion processes. These regions may be associated with boundaries and can also be moving about in time. The accuracy and efficiency of the adaptive finite-element method are compared with those of finite-difference and non-adaptive finite-element procedures.

Governing Equations

The conservation equations for multicomponent reacting ideal mixtures in one-dimensional Cartesian coordinates can be written as follows[10]

Continuity

$$\frac{\partial \rho}{\partial t}+\frac{\partial}{\partial x}(\rho u)=0 \tag{1}$$

Momentum

$$\rho\left[\frac{\partial u}{\partial t}+u\frac{\partial u}{\partial x}\right]=-\frac{\partial p}{\partial x}+\frac{\partial}{\partial x}\left(\frac{4}{3}\mu\frac{\partial u}{\partial x}\right) \tag{2}$$

Energy

$$\rho C_p\left[\frac{\partial T}{\partial t}+u\frac{\partial T}{\partial x}\right]=\frac{\partial p}{\partial t}+u\frac{\partial p}{\partial x}+\frac{\partial}{\partial x}\left(\mu C_p\frac{\partial T}{\partial x}\right)+\frac{4}{3}\mu\left(\frac{\partial u}{\partial x}\right)^2-\sum_{j=1}^{N}H_j\dot{m}_j+\sum_{j=1}^{N}\rho D C_{p_j}\frac{\partial T}{\partial x}\frac{\partial y_j}{\partial x} \tag{3}$$

Species

$$\rho\left[\frac{\partial y_j}{\partial t}+u\frac{\partial y_j}{\partial x}\right]=\dot{m}_j+\frac{\partial}{\partial x}\left(\rho D\frac{\partial y_j}{\partial x}\right)\qquad j=1,\ldots,N-1 \tag{4}$$

$$y_N=1-\sum_{m=1}^{N-1}y_j \tag{5}$$

State

$$p=\rho\tilde{R}T\sum_{j=1}^{N}\frac{y_j}{W_j} \tag{6}$$

where

$$C_p=\sum_{j=1}^{N}y_jC_{p_j} \tag{7}$$

and

$$H_j=H_j^0+\int_{T_0}^{T}C_{p_j}\mathrm{d}t \tag{8}$$

In deriving these equations we have neglected the thermal diffusion of the species (the Soret and Dufour effects), the pressure gradient diffusion, the bulk viscosity, and radiation heat transfer. In addition, the Prandtl number was assumed equal to one, and the species were assumed to diffuse according to Fick's law with equal diffusion coefficients for all of them.

In enclosed deflagrations, the Mach number is small and the pressure is almost spatially uniform, i.e., $p=p(t)$. Under this assumption, the momentum equation and the viscous dissipation term in the energy equation can be dropped. Furthermore, by assuming that the species specific heats at constant pressure are equal and constant, and that the Lewis number is unity, Eq. (3) can be written as

$$\rho C_p\left[\frac{\partial T}{\partial t}+u\frac{\partial T}{\partial x}\right]=\frac{dp}{dt}+C_p\frac{\partial}{\partial x}\left(\rho D\frac{\partial T}{\partial x}\right)-\sum_{j=1}^{N}H_j^0\dot{m}_j \tag{9}$$

Equation (9) can be further simplified by assuming that the species specific heats at constant volume are equal and constant. This implies that the ratio of specific heats, $\gamma=C_p/C_v$, is also a constant and the species molecular weights are equal and will be denoted by W. These assumptions allow us to introduce the following transformation

$$\phi=Tp^{(1-\gamma)/\gamma} \tag{10}$$

into Eq. (9) to yield

$$\rho\left[\frac{\partial \phi}{\partial t}+u\frac{\partial \phi}{\partial x}\right]=\frac{\partial}{\partial x}\left(\rho D\frac{\partial \phi}{\partial x}\right)-\sum_{j=1}^{N}H_j^0\dot{m}_j\Big/C_pp^{(\gamma-1)/\gamma} \tag{11}$$

Equations (4) and (11) represent a set of convection-reaction-diffusion equations which can be further simplified by introducing the following Spalding's Lagrangian transformation[1]

$$\rho=M\frac{\partial \xi}{\partial x} \tag{12}$$

and

$$\rho u=-M\frac{\partial \xi}{\partial t} \tag{13}$$

where

$$M=\int_0^L\rho\mathrm{d}x \tag{14}$$

In Eq. (14), M denotes the mass (per unit area) contained in a closed combustor of length L and is a constant.

The purpose of the Lagrangian transformation introduced before is to eliminate the continuity equation [Eq. (1)] and the convection terms from Eqs. (4) and (11). Thus, introducing Eqs. (12) and (13) into Eqs. (4) and (11) and assuming that ρ^2D is constant, the equations governing the propagation of laminar flames in the domain $0\le x\le L$ (or $0\le\xi\le 1$) can be written as

$$\frac{\partial y_j}{\partial t}=\alpha\frac{\partial^2 y_j}{\partial \xi^2}+\dot{\omega}_j,\qquad j=1,\ldots,N-1 \tag{15}$$

$$y_N = 1 - \sum_{j=1}^{N-1} y_j \tag{16}$$

and

$$\frac{\partial \phi}{\partial t} = \alpha \frac{\partial^2 \phi}{\partial \xi^2} - \sum_{j=1}^{N} H_j^0 \dot{\omega}_j \Big/ C_p p^{(\gamma-1)/\gamma} \tag{17}$$

where

$$\alpha = \rho^2 D / M^2 \tag{18}$$

and

$$\dot{\omega}_j = \dot{m}_j / \rho \tag{19}$$

The value of $\rho^2 D$ was taken equal to 2.1718×10^{-7} g^2/cm^4/s and corresponds to that of air at atmospheric pressure and 300 K. Under those conditions the value of D is 0.1567 cm^2/s.

It should be pointed out that the assumption of constant C_p and C_v, and Lewis number equal to one, are essential to the formulation of Eqs. (15) and (17). If the assumption of constant C_p and C_v were relaxed, the transformation given by Eq. (10) would still be valid. However, Eq. (17) would contain terms proportional to the derivatives of γ with respect to t and ξ. A constant value of the Lewis number can easily be incorporated in our present model since it only requires the modification of the diffusion coefficient, α, in Eq. (15). The diffusion coefficient would become the value of the previous diffusion coefficient divided by the Lewis number.

The assumption of a constant value of $\rho^2 D$ can also be relaxed in our model. A nonconstant value of $\rho^2 D$ would imply that the diffusion coefficient is nonconstant and that the diffusion terms in Eqs. (15) and (17) are $\partial(\alpha \partial Y_j/\partial \xi)/\partial \xi$ and $\partial(\alpha \partial \phi/\partial \xi)/\partial \xi$, respectively.

Once the value of ϕ is calculated from Eq. (17), the pressure can be calculated by substituting the value of T from Eq. (10) into Eq. (6) and integrating the resulting equation. This yields

$$p^{(1/\gamma)} L = RM \int_0^1 \phi \, d\xi \tag{20}$$

where $R = \tilde{R}/W$.

The temperature can then be obtained from Eq. (10). The density is calculated from Eq. (6) using the value of the temperature given by Eq. (10). This results in

$$\rho = p^{(1/\gamma)} / R\phi \tag{21}$$

Equations (15) and (17) represent a system of three integrodifferential reaction-diffusion equations (cf. next section) which can be written in vector form as

$$\frac{\partial A}{\partial t} = \alpha \frac{\partial^2 A}{\partial \xi^2} + S \tag{22}$$

where

$$A = (y_1, y_2, \phi)^T \qquad S = \left(\dot{\omega}_1, \dot{\omega}_2, -\frac{Q\dot{\omega}_1}{C_p p^{(\gamma-1)/\gamma}}\right)^T \tag{23}$$

and

$$\sum_{j=1}^{N} H_j^0 \dot{\omega}_j = Q\dot{\omega}_1 \tag{24}$$

The integrodifferential nature of Eq. (22) is due to the dependence of p on ϕ given by Eq. (20). The solution of Eq. (22) yields the values of y_1, y_2, and ϕ in terms of Lagrangian coordinates ξ and time t. The profiles of these variables and the temperature can be obtained in terms of the physical coordinate x by integrating Eq. (12) as follows

$$x = M \int_0^{\xi} \frac{d\xi}{\rho} \tag{25}$$

The velocity can be calculated from Eqs. (1) and (12) and is given by the following expression

$$u = -\frac{1}{\rho} \int_0^x \frac{\partial \rho}{\partial t} \, dx \tag{26}$$

Chemical Reaction

In the present study a one-step irreversible chemical reaction of the Arrhenius type has been considered

$$\underset{\text{(Species 1)}}{\text{Fuel}} + \underset{\text{(Species 2)}}{\text{Oxidizer}} + \underset{\text{(Species 3)}}{\text{Inert}} \rightarrow \underset{\text{(Species 4)}}{\text{Products}} + \text{Inert} \tag{27}$$

Thus, $N=4$. For a homogeneous premixed mixture the inert mass fraction, y_3, is constant in space and time, and the products mass fraction is given by Eq. (16). This means that only the equations for the fuel and oxidizer mass fractions and the ϕ equation need to be solved. The values of the reaction rate terms $\dot{\omega}_j$ are

$$\dot{\omega}_1 = -K \exp\left(-\frac{E}{\tilde{R}T}\right) \rho y_1 y_2 \tag{28}$$

$$\dot{\omega}_2 = s\dot{\omega}_1 \tag{29}$$

where $K = 3.12 \times 10^{11}$ cm^3/g/s, $s = 3.63$, $Q = 11{,}070$ cal/g, and $E = 30{,}000$ cal/mole. The values of the constants K, s, Q, and E are typical of hydrocarbons. The stoichiometric coefficient s corresponds to the complete oxidation of propane/air mixtures to carbon dioxide, water vapor, and nitrogen. The heat of reaction Q is that of propane at 300 K, while the activation energy E was obtained from the shock tube experiments performed by Myers and Bartle.[11] The preexponential factor K has the value of 10^{13} cm^3/mole^2/s.

Initial and Boundary Conditions

Initially the velocity was set to zero and the pressure was 1 atm. The species and temperature profiles were given by the following expressions

$$\left.\begin{aligned} T(0,\xi) &= 1500 \text{ K} \\ y_1(0,\xi) &= 0.01 \\ y_2(0,\xi) &= 0.03652 \end{aligned}\right\} \qquad 0 \le \xi \le 0.0438 \tag{30}$$

$$\left.\begin{aligned} T(0,\xi) &= 300 \text{ K} \\ y_1(0,\xi) &= 0.06472 \\ y_2(0,\xi) &= 0.23550 \end{aligned}\right\} \qquad 0.0938 \le \xi \le 1.0 \tag{31}$$

and

$$y_3(t,\xi) = y_3(0,\xi) = 0.69978 \qquad 0 \le \xi \le 1 \tag{32}$$

Linear temperature and species mass fraction profiles were assumed for $0.0438 \le \xi \le 0.938$.

Equations (31) and (32) correspond to the presence of burnt gases at the combustor left end. Thus, we do not consider here the ignition phenomenon. It is to be noted that the initial

conditions correspond to a stoichiometric mixture of fuel and oxidizer, and that the mass fraction of oxidizer [given by Eqs. (30) and (31)] was calculated using these stoichiometric conditions.

The combustor ends were assumed adiabatic and the following boundary conditions were applied

$$\frac{\partial A}{\partial \xi}(t,0) = \frac{\partial A}{\partial \xi}(t,1) = 0 \tag{33}$$

Given the initial pressure and temperature profiles the density can be calculated from Eq. (6). Then, the mass contained in the combustor can be calculated from Eq. (25). This results in

$$M = L \Big/ \int_0^1 \frac{d\xi}{\rho} \tag{34}$$

Finite-Element Method

The solution of Eq. (22) was obtained using a semidiscrete Galerkin method which uses a finite-element approximation in space and finite differences in time. A brief discussion of the method is presented here.

Let us define $\psi_j(\xi)$, $j=1,\ldots,n$ as the spatial basis used in the finite-element method, where n is the number of grid points and ψ_j are the roof functions which are defined as

$$\psi_j = 0 \quad \text{for} \quad \xi \geq \xi_{j+1} \quad \text{and} \quad \xi \leq \xi_{j-1} \tag{35}$$

$$\psi_j = 1 \quad \text{at} \quad \xi = \xi_j \tag{36}$$

and ψ_j varies linearly between ξ_{j-1} and ξ_j, and ξ_j and ξ_{j+1}.

Multiplying Eq. (22) by ψ_j, integrating the resulting equation between $\xi=0$ and $\xi=1$, and applying the boundary conditions given by Eq. (33), we obtain

$$\int_0^1 \frac{\partial A}{\partial t}\psi_j d\xi = -\alpha \int_0^1 \frac{\partial A}{\partial \xi}\frac{\partial \psi_j}{\partial \xi} d\xi + \int_0^1 S\psi_j d\xi \tag{37}$$

The vector of dependent variables A is written as a linear combination of the linear basis as

$$A = \sum_{\ell=1}^{n} q_\ell(t)\psi_\ell(\xi) \tag{38}$$

which, when substituted into Eq. (37), yields

$$\sum_{\ell=1}^{n} (a_{\ell_j}\dot{q}_\ell + \alpha b_{\ell_j} q_\ell) = \int_0^1 S\psi_j d\xi \tag{39}$$

where

$$a_{\ell_j} = \int_0^1 \psi_\ell \psi_j d\xi \tag{40}$$

and

$$b_{\ell_j} = \int_0^1 \frac{\partial \psi_\ell}{\partial \xi}\frac{\partial \psi_j}{\partial \xi} d\xi \tag{41}$$

Equation (39) represents a system of ordinary differential equations for q_ℓ, i.e., it represents a system of n first order ordinary differential equations whose unknowns are q_ℓ. These differential equations were discretized using a trapezoidal rule at $t^{(n+1/2)}$ to yield the following system of algebraic equations:

$$\sum_{\ell=1}^{N}\left[a_{\ell_j}\frac{q_\ell^{(n+1)} - q_\ell^{(n)}}{\Delta t} + \frac{\alpha}{2} b_{\ell_j}(q_\ell^{(n)} + q_\ell^{(n+1)})\right] = \frac{1}{2}\left[\int_0^1 S^{(n)}\psi_j d\xi + \int_0^1 S^{(n+1)}\psi_j d\xi\right] \tag{42}$$

The reaction terms S_{y_1} $(=\dot{\omega}_1)$ and S_{y_2} $(=\dot{\omega}_2)$ are linear in y_1 and y_2, respectively, while S_ϕ is nonlinear in ϕ. The terms $S_{y_1}^{(n+1)}$ and $S_{y_2}^{(n+1)}$ were not linearized when solving Eq. (42). The term S_ϕ given by Eq. (23) depends on y_1, y_2, ρ, ϕ, and p, where p and ρ in turn depend on ϕ only. This term was first written as a function of y_1, y_2, p, and ϕ and linearized only with respect to ϕ. It was not linearized with respect to p despite the fact that the pressure is only a function of ϕ [Eq. (20)]. Thus, $S_\phi^{(n+1)}$ was linearized to yield

$$S_\phi^{(n+1)} = S_\phi^{(n)} + \frac{\partial S_\phi^{(n)}}{\partial \phi}(\phi^{(n+1)} - \phi^{(n)}) \tag{43}$$

Since the nonlinear terms S_{y_1} and S_{y_2} were not linearized, and no linearization of S_ϕ with respect to p was performed, the pressures S_{y_1} and S_{y_2} were solved using an iterative procedure. It should be pointed out that the linearization of S_ϕ with respect to p was not performed because of the integral dependence of p on ϕ given by Eq. (20). This integral constraint is the reason for the requirement of an iterative procedure. Numerical experiments showed that the convergence rate of the finite-element method could be accelerated if the source S_ϕ were linearized. This linearization is given by Eq. (43) and was used to solve Eq. (22).

Convergence within the time step was established when the L_2 norm, defined by

$$L_2 = \sqrt{\sum_{i=1}^{n} |(A_i^2)^{(k+1)} - (A_i^2)^{(k)}|/n} \tag{44}$$

was less than or equal to 10^{-4}.

Presentation and Discussion of Results

The linear finite-element method described above was first applied to compute the steady-state wave speed of a reaction-diffusion equation which has an exact traveling wave solution and then used to study the propagation of laminar flames using the Lagrangian formulation described before. The results of these computations are presented in the next three subsections.

Application of the Finite-Element Method to Reaction-Diffusion Equations

The Fisher equation[9] was chosen as a model equation because it has an exact traveling wave solution with which the numerical results can be compared. This equation can be written in nondimensional variables as

$$\frac{\partial A}{\partial t} = \frac{\partial^2 A}{\partial \xi^2} + A(1-A) \tag{45}$$

where A stands for a scalar $(0 \leq A \leq 1)$. The solution of the Fisher equation in the interval $-\infty < \xi < \infty$ can be written as

$$u(\xi,t) = 1/\{1+\exp[(\xi - Vt)/\sqrt{6}]\}^2 \tag{46}$$

where V is the wave speed and is equal to $5/\sqrt{6}$. Equation (45) was numerically solved in the domain $-50 \leq \xi \leq 400$ using an equally-spaced grid. This truncation of the infinite domain $(-\infty < \xi < \infty)$ was found sufficient to eliminate boundary effects.

The following boundary and initial conditions were applied

$$\frac{\partial A}{\partial \xi}(-50,t) = \frac{\partial A}{\partial \xi}(400,t) = 0 \tag{47}$$

and

$$A(\xi,0) = 1/[1+\exp(\xi/\sqrt{6})]^2 \tag{48}$$

Figure 1 presents the computed wave speed,

$$V_c = \int_{-50}^{400} A(1-A)\,d\xi \tag{49}$$

using the finite-element method and the Crank-Nicolson finite-difference scheme for two grids with 451 and 901 points, respectively. In these calculations, the reaction term $A(1-A)$ was not time-linearized, and the system of algebraic equations was solved using an iterative procedure. Convergence within the time step was established using the L_2 norm defined in Eq. (44). The wave speed was obtained by assuming a steadily propagating traveling wave, i.e., $\partial A/\partial t = -V(\partial A/\partial \xi)$, and integrating Eq. (45) from $\xi = -50$ to $\xi = 400$.

The computations with a 451-point grid were performed with $\Delta t = 0.2$, while those with 901 points were performed with $\Delta t = 0.05$.

It is clear from Fig. 1 that the Crank-Nicolson scheme overpredicts the steady state wave speed, whereas the finite-element method underpredicts it. For a 451-point grid the wave speed computed with the Crank-Nicolson algorithm is more accurate than that computed with the finite-element method. The reverse is true for a 901-point grid. For 451 equally-spaced grid points and $\Delta t = 0.2$, the computations performed with the Crank-Nicolson and finite-element methods required 163 and 171 seconds of CPU time in a DEC-2060 computer.

Application of an Adaptive Finite-Element Method to Reaction-Diffusion Equations

The results presented in the previous subsection show that, in order to obtain an accurate wave speed for the Fisher equation, a large number of points are required if an equally-spaced grid is used. For $\Delta t = 0.2$, for example, the wave speed computed with 451 and 901 points differs by 4% and 0.4%, respectively, from the exact wave speed at $t = 20$. The calculations performed with 901 points required 252 seconds of CPU time in a DEC-2060 computer.

The wave front of the Fisher equation is relatively a thin region compared to the length of the computational domain. In an equally-spaced grid, points located away from the wave front do not contribute to the computed wave speed. Thus, the use of an adaptive finite-element method that concentrates

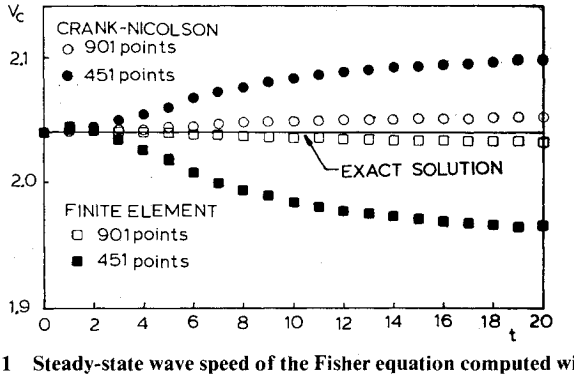

Fig. 1 Steady-state wave speed of the Fisher equation computed with the Crank-Nicolson and finite-element methods.

most of the grid points at the wave front, while using few points before and behind it, seems to offer a promising approach for improving efficiency without losing accuracy.

Adaptive grid techniques for finite-difference schemes have been investigated by Dwyer[12] and Dwyer and Sanders.[13] They used a transformation of coordinates technique which concentrates the grid points in the steepest temperature gradient regions. In addition, they also collocated the new grid using Lagrange and spline interpolation for the values of the dependent variables. Our adaptive finite-element technique, however, uses a projection method.[14] The method is based on the known solution at time $t^{(n)}$ which can be written as a sum of linear basis [Eq. (38)]. Thus, the solution vector at time $t^{(n)}$ can be expressed as

$$A^{(n)} = \sum_{j=1}^{n} a_j^{(n)} \psi_j^{(n)}(\xi) \tag{50}$$

where $\psi_j^{(n)}$ are the linear basis at time $t^{(n)}$. The new grid at $t^{(n+1)}$ is determined according to the steepest temperature gradient, which defines a new set of linear basis, $\psi_j^{(n+1)}(\xi)$. To advance the solution $t^{(n)}$ to $t^{(n+1)}$, the initial conditions are defined as

$$A^{(*)} = \sum_{i=1}^{n} b_i^{(n)} \psi_i^{(n+1)}(\xi) \tag{51}$$

In Eq. (51), the $b_i^{(n)}$ are determined by minimizing the following functional

$$\tfrac{1}{2}(A^{(*)},A^{(*)}) - (A^{(n)},A^{(*)}) \tag{52}$$

where the inner product is given by, for example,

$$(A^{(n)},A^{(*)}) = \int_0^1 A^{(n)} A^{(*)}\,d\xi \tag{53}$$

Although the elements can be moved with the computed wave speed at every time step,[14] in practice their adaptation is exercised at some fixed time intervals. For the Fisher equation whose exact wave speed is known, we simply placed enough points to cover the wave front and the elements were moved, i.e., adapted, every 10 time steps. Table 1 shows a comparison between the equally-spaced, i.e., fixed, grid points and the adaptive finite-element methods for a particular case of $\Delta t = 0.2$. This comparison shows that the adaptive method can achieve the same accuracy, while drastically reducing the execution time and storage requirements, as the nonadaptive finite-element method.

Application of the Finite-Element Method to One-Dimensional Flame Propagation Problems

In this section, Eq. (22) is solved using the finite-element method. Calculations were also performed using the Crank-Nicolson scheme but are not reported here. The largest temperature difference between these two methods is less than 2% and could not be distinguished when plotted in Figs. 2-6.

In Fig. 2 we show the temperature profiles vs the Lagrangian coordinate ξ at different times. It is clear from this figure that the flame propagates from left to right and is characterized by a steep temperature gradient. The temperature of the unburnt and burnt gases increases due to the pressure rise and the adiabatic compression of the burnt gases. At $t = 0.90$ s the stoichiometric mixture is fully burned and diffusion tends to homogenize the temperature throughout the combustor length. It should be noted that the calculations reported here were performed with $\Delta t = 10^{-5}$ s and 401 points. Between five and seven of these grid points were located at the flame front.

The choice of $\Delta t = 10^{-5}$ s was based on numerical experiments which were performed in a 401-point grid. These experiments were intended to assess the influence of the time step on the linearization of the reaction terms and the solution. The time step was also selected in such a way that the temperature differences between the finite-difference and finite-element methods were always less than 2.5% of the temperature computed with the Crank-Nicolson scheme.

Figure 3 presents the fuel mass fraction profiles vs the Lagrangian coordinate ξ at different times. The flame propagates from left to right in this figure and its thickness decreases with time due to the pressure rise and the reaction rate increase. The pressure profile vs time is presented in Fig. 4 and shows that the pressure is a monotonically increasing function of time until the flame reaches the right end of the combustor. Afterwards, the pressure remains constant due to the absence of chemical reaction and the spatial temperature variations disappear because of the diffusion.

In Figs. 5 and 6 we show the temperature and fuel mass fraction profiles vs the x coordinate at different times. The x coordinate was calculated from Eq. (25) using the trapezoidal rule. These figures indicate that the flame accelerates from $t = 0$ to $t = 0.20$ s and then decelerates.

As we mentioned before, the calculations performed using the Crank-Nicolson scheme are in good agreement with those obtained with the present semidiscrete Galerkin method. The maximum temperature difference between these two methods was less than 2%. This difference is in part due to the different convergence criteria used in the two methods: the convergence criterion for the finite-element method was the L_2 norm defined by Eq. (44) and the Crank-Nicolson scheme was said to converge whenever

$$|T_i^{(k+1)} - T_i^{(k)}|/T_i^{(k)} \leq 10^{-4} \text{ and } |p^{(k+1)} - p^{(k)}|/p^{(k)} \leq 10^{-4} \tag{54}$$

Equation (54) represents local convergence criteria, whereas that of Eq. (44) is a global criterion. It should be pointed out that in the Crank-Nicolson scheme no linearization was carried out with respect to time and that the finite-difference equations were solved using an iterative procedure and a tridiagonal matrix algorithm.[1]

Other possible reasons which account for the 2% maximum temperature difference between the Crank-Nicolson and the finite-element methods are the linearization of the reaction term S_ϕ and the linear basis ψ_j used in the finite-element scheme. The time linearization of the highly nonlinear reaction terms certainly reduces the accuracy of the present transient calculations if the time step used in the computations is not small enough or if the reaction terms are very nonlinear as in the present case. For example, Ramos[1] has recently shown that a quasilinear method requires smaller time steps than a Crank-Nicolson scheme to obtain almost identical solutions.

Although we have used linear basis for computational reasons, it should be noted that at the flame front where very steep temperature gradients exist it may be necessary to use higher order basis and even Hermite polynomials. However, this was not investigated in the present work. Furthermore, it is worth noting that the solutions obtained with the finite-element method show oscillations in the temperature field for the burnt and unburnt gases. Fortunately, these oscillations did not grow in time and were less than 0.3% of peak temperature in our computations. These oscillations, however, affect the pressure [see Eqs. (10) and (20)] and the reaction rates and may account somewhat for the differences mentioned before. No oscillations were observed in the Crank-Nicolson scheme results. This is because finite-difference schemes generally give rise to smooth solutions since they are based on Taylor series expansions and the functions need to be continuous and differentiable up to the highest order derivative which appears in the differential equation. In contrast, the finite-element method does not require the existence of higher order derivatives or the continuity of the functions. However, the method does require that the integrals of Eqs. (40-42) exist. This means that the functions must be integrable in a suitable normed space, e.g., a Sobolev space.

This is a major difference between finite-difference and finite-element methods which in the present study may be interpreted as temperature oscillations in the finite-element method.

The fact that finite-difference schemes require that the functions be differentiable up to the highest order of the differential equation implies that the truncation errors of these schemes can be obtained explicitly using Taylor series expansions of the finite-difference equations. In contrast, the finite-element method does not have truncation errors because the finite-element equation cannot, in general, be expanded in Taylor series. This is compensated by using norms such as the L_2 norm introduced in Eq. (44).

Although these differences between the finite-element and finite-difference schemes are important, one cannot conclude that finite-element methods are better (or worse) than finite-difference schemes. For example, in order to deal with the presence of irregular geometries, finite-element methods are by far superior to finite-difference schemes. Furthermore, as we have already seen in the temperature profiles and Fig. 1, nonlinear terms are apparently better accounted for by the finite-element method. Thus, highly nonlinear terms seem to be resolved better by the finite-element algorithm than by the finite-difference scheme.

For a given accuracy, the finite-element method is as efficient as the Crank-Nicolson scheme employed in this study (see also Ref. 1). It should be pointed out, however, that the Fisher equation and the propagation of confined laminar flames are relatively simple, although nonlinear problems. Thus, our conclusions about the efficiency and accuracy of finite-difference and finite-element methods may not hold for more complicated, e.g., multidimensional flow configurations. At most our results indicate that the finite-element method seems to offer a promising alternate procedure to finite-difference algorithms, and that finite-element schemes should be further explored. We are presently investigating ignition and unconfined flame propagation problems in order to establish whether this paper's conclusions are applicable to other combustion problems.

Furthermore, the results of these calculations have shown that for a combustor length of 10 cm 401 grid points are required to have five to seven points in the flame front. Computations were also performed using 82 grid points and showed that in this case at most three grid points were located at the flame front. Obviously three grid points are inadequate to predict the formation of radicals at the flame front when complex chemical kinetics schemes are used. Thus, we can easily conclude that in order to predict the formation of radicals and minor species occurring in a 10 cm long combustor using an equally-spaced grid, at least 401 points are required. However, it is to be expected that most of the computation time will be spent in calculating the highly nonlinear reaction terms, when in fact the region where most of the physical changes take place is the flame front. Thus, the use of an adaptive finite-element technique that concentrates most of the grid points at the flame front while using very few points in the unburnt and burnt gas regions which have almost uniform temperature fields, seems to offer a promising approach.

The application of the adaptive finite-element method to the propagation of confined laminar flames is presently under study. However, at the present it is not clear whether the accuracy and convergence properties of the adaptive finite element which were obtained for constant wave speed problems[14] are still valid for the case of confined laminar flames whose velocity is not constant.

Table 1 Comparison between adaptive and nonadaptive finite-element methods

	Equally-spaced grid		Adaptive grid[a]	
Total No. of points	451	901	101	171
No.of points in wave front	70	140	70	140
Wave speed at $t=20$	1.9654908	2.0330674	1.9675210	2.0330397
CPU time, s	171	252	24	30

[a] 11 and 20 points are located behind and before the flame front, respectively.

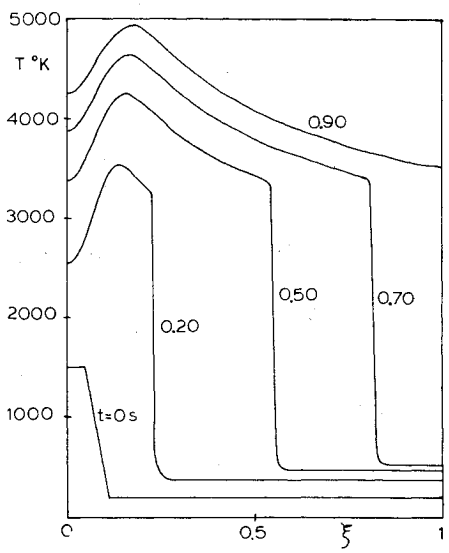

Fig. 2 Temperature profiles vs the Lagrangian coordinate at different times.

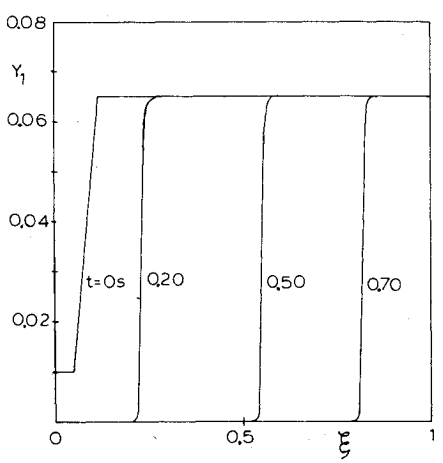

Fig. 3 Fuel mass fraction profiles vs the Lagrangian coordinate at different times.

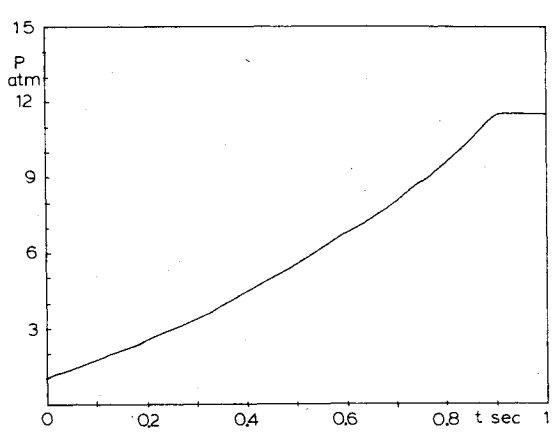

Fig. 4 Pressure vs time.

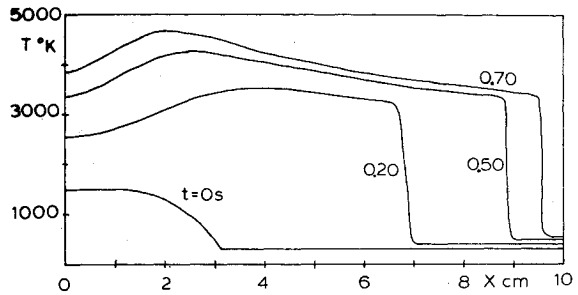

Fig. 5 Temperature profiles vs the Eulerian coordinate at different times.

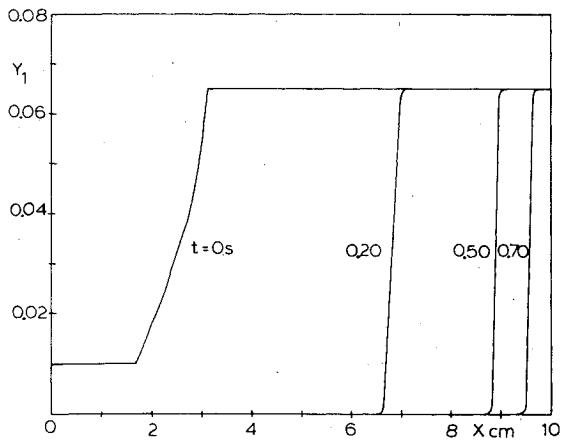

Fig. 6 Fuel mass fraction profile vs the Eulerian coordinate at different times.

Conclusions

A semidiscrete Galerkin finite-element method which uses linear basis in space and trapezoidal finite-differences in time has been developed and applied to study the propagation of laminar flames in a one-dimensional closed combustor. The governing equations have been solved in Lagrangian coordinates. The numerical results show that a maximum of 2% temperature difference exists between the Crank-Nicolson and the finite-element schemes. These differences can be attributed to the linear basis of the method, the time linearization of the reaction terms and very small temperature oscillations. These oscillations are typical in the finite-element method, although they do not grow with time, and are about 0.3% of the peak temperature value for the problem studied.

The finite-element method has also been used to calculate the wave speed of the Fisher equation which has an exact traveling wave solution. The finite-element results are compared to those obtained with a Crank-Nicolson scheme and show that while the finite-element method underpredicts the steady state wave speed, the Crank-Nicolson scheme overpredicts it. For a 901-point grid, the wave speed computed with the finite-element algorithm is closer to the exact wave speed than that obtained using the Crank-Nicolson method.

An adaptive finite-element method has also been developed and applied to calculate the Fisher equation wave speed. The results indicate that in order to get the same accuracy as the Galerkin method with 901 points, the adaptive finite-element method requires only 171 points. The adaptive method is approximately seven times more efficient than the Galerkin method.

Acknowledgment

The first author was partially supported by the Army Research Office, Grant DAAG 29-80-C-0081.

References

[1] Ramos, J. I., "A Numerical Study of One-Dimensional Enclosed Flames," *Numerical Properties and Methodologies in Heat Transfer: Proceedings of the 2nd National Symposium*, Hemisphere Pub. Co., Washington, D.C., 1982, pp. 529-546.

[2] Ramos, J. I., "Numerical Studies of Laminar Flame Propagation in Spherical Bombs," AIAA Paper 82-0038, Jan. 1982.

[3] Ramos, J. I., "Numerical Studies of One-Dimensional Unsteady Flame Propagation," *Proceedings of the 10th IMACS World Congress on System Simulation and Scientific Computation*, IMACS, 1982, pp. 164-166.

[4] Margolis, S. B., "Time-Dependent Solution of a Premixed Laminar Flame," *Journal of Computational Physics*, Vol. 27, June 1978, pp. 410-427.

[5] Otey, G. R. and Dwyer, H. A., "A Numerical Study of the Interaction of Fast Chemistry and Combustion," *AIAA Journal*, Vol. 17, June 1979, pp. 606-613.

[6] Heimerl, J. M. and Coffee, T. P., "The Detailed Modeling of Premixed, Laminar Steady-State Flames. I: Ozone," *Combustion and Flame*, Vol. 39, Nov. 1980, pp. 301-315.

[7] Madsen, B. K. and Sincovec, R. F., "PDECOL: General Collocation Software for Partial Differential Equations," Lawrence Livermore Laboratory, Livermore, Calif., Preprint UCRL-78263 (Rev. 1), 1977.

[8] Sandusky, H., Bellan, J. R., Ohlemiller, T. J., and Vichnevetsky, R., "Linear Finite Element Numerical Techniques for Combustion Problems Requiring Variable Step Size," *Combustion and Flame*, Vol. 36, Oct. 1979, pp. 193-196.

[9] Reitz, R. D., "The Application of an Explicit Numerical Method to a Reaction-Diffusion System in Combustion," The Courant Institute of Mathematical Sciences, New York, 1979.

[10] Williams, F. A., *Combustion Theory*, Addison-Wesley Publishing Co., Reading, Mass., 1965, pp. 1-17.

[11] Myers, B. F. and Bartle, E. R., "Reaction and Ignition Times on the Oxidation of Propane," *AIAA Journal*, Vol. 7, Oct. 1969, pp. 1862-1869.

[12] Dwyer, H. A., "A Generalized Adaptive Grid Method for Heat Transfer," First National Conference on Numerical Methods in Heat Transfer, Univ. of Maryland at College Park, Md., 1979, pp. 50-70.

[13] Dwyer, H. A. and Sanders, B. R., "Numerical Modeling of Unsteady Flame Propagation," Sandia National Laboratories, Livermore, Calif., Report No. SAND77-8275, 1977.

[14] Fix, G. J., Lee, D. N., and Ramos, J. I., "Adaptive Finite-Element Methods for Initial Value Problems," Department of Mathematics, Carnegie-Mellon Univ., Pittsburgh, Pa., 1982.